Reactive & Functional Polymers 71 (2011) 553–560

Contents lists available at ScienceDirect

Reactive & Functional Polymers

journal homepage: www.elsevier.com/locate/react

Synthesis and photoresponsive behaviors of novel poly(arylene ether)s with di-azobenzene pendants

Jingjing Zhang [a], Haibo Zhang [a], Xingbo Chen [a,b], Jinhui Pang [a], Yuxuan Zhang [a], Yongpeng Wang [a], Qidai Chen [c], Songhao Pei [d], Weixian Peng [d], Zhenhua Jiang [a,*]

[a] Alan G. MacDiarmid Institute, Jilin University, Changchun 130012, China
[b] State Key Lab for Ceramic Fibers Composites, National University of Defense Technology, Changsha, Hunan 410073, China
[c] State Key Lab on Integrated Optoelectronics, College of Electronic Science and Engineering, Jilin University, Changchun 130012, China
[d] College of Physics, Jilin University, Changchun 130012, China

ARTICLE INFO

Article history:
Received 26 October 2010
Received in revised form 21 January 2011
Accepted 24 January 2011
Available online 1 February 2011

Keywords:
Poly(arylene ether)s
Di-azobenzene
Photoinduced birefringence
Surface relief gratings

ABSTRACT

Novel poly(arylene ether)s containing di-azobenzene moieties (diazo-PAEs) were synthesized from a new di-azobenzene monomer, bis(4-((4-cyanophenyl)diazenyl)phenyl)5,5′-carbonylbis(2-fluorobenzenesulfonate). These polymers show good thermal stability, with glass transition temperatures and 5% weight-loss temperatures above 160 °C and 406 °C, respectively. Upon irradiation with a 532 nm neodymium dope yttrium aluminum garnet (Nd:YAG) laser beam, these polymers present a high remnant value, and no fatigue phenomena were observed after several cycles of inscription–erasure–inscription sequences. By exposing diazo-PAE films to an interference pattern of laser beams (355 nm) at modest intensity (approximately 80 mW/cm^2), stable surface relief gratings (SRGs) can be formed.

1. Introduction

Polymers containing azobenzene units in main chains or as pendant groups along the backbone have been attracting a great deal of attention because of their potential applications in optical data storage, optical switches, and electro-optical modulators [1–7]. Azo-polymers have many attractive features, especially their unique reversible photoisomerization and the anisotropy of the azobenzene chromophores. The photoisomerization can cause significant changes in the bulk properties, surface properties and polarity of the polymers. One of the attractive phenomena is photoinduced birefringence in films when they are irradiated by linearly polarized light. When excited by linearly polarized laser light, the chromophores undergo *trans–cis-trans*-isomerization accompanied by molecular reorientation. Through the hole-burning mechanism, an excess of chromophores occurs in the direction perpendicular to the laser polarization. This molecular reorientation induces birefringence, and this reorientation can be reversed by irradiation with circularly polarized light or depolarized light [8]. Another active field of azo-polymer research is the investigation of surface relief gratings (SRGs) formed directly on the polymer films by exposing the films to an interfering laser beam [9,10]. These SRGs are stable below the glass transition temperatures (T_gs) of the polymers and can be removed by heating the polymers above their T_gs or can be erased optically. Although the understanding of the mechanism responsible for SRG formation is still evolving, this phenomenon has already been explored in various azobenzene-containing systems, including amorphous polymers [11], liquid crystalline polymers [12,13], molecular glasses [14–16], and supramolecular polymers [17,18].

In recent years, azobenzene chromophores have been introduced into some high-T_g aromatic polymers such as azo-PI and azo-PU because this strategy is helpful to improve the stability of azobenzene chromophores for optical storage applications [11,19,20]. Poly(arylene ether)s (PAEs) are high-performance thermoplastics that are well known for their excellent thermal, mechanical, and environmental stabilities. These materials can be used in a wide range of demanding applications from aerospace to microelectronics [21]. Functionalized poly(arylene ether)s have received much attention due to their potential applications in proton-exchange membranes, light-emitting materials, and optical materials [22–25]. In our previous work, we synthesized some photoresponsive azo-poly(arylene ether)s by direct copolymerization and investigated their corresponding optical properties [26–28]. These azo-PAEs display photoinduced birefringence behavior with a high remnant value, and stable SRGs can be formed on them. However, most azo-PAEs have relatively low molecular weights and intrinsic viscosities below 0.3 dL/g due to the low reactivity of azo-monomers. In this work, we synthesized a new

* Corresponding author. Tel./fax: +86 0431 85168886.
E-mail address: jiangzhenhua@mail.jlu.edu.cn (Z. Jiang).

1381-5148/$ - see front matter © 2011 Elsevier Ltd. All rights reserved.
doi:10.1016/j.reactfunctpolym.2011.01.011

bifluoride monomer with two azobenzene units, bis(4-((4-cyanophenyl)diazenyl)phenyl)5,5′-carbonylbis(2-fluorobenzenesulfonate) (monomer 2). From this monomer, novel poly(arylene ether)s with di-azobenzene pendants (diazo-PAEs) were prepared by nucleophilic aromatic substitution polymerization. The thermal and optical properties of the diazo-PAEs were also investigated.

2. Experimental

2.1. Materials

4-Aminobenzonitrile and 4,4′-(hexafluoroisopropylidene) diphenol (6F-BPA) were purchased from Alfa Aesar. 4,4′-Difluorobenzophenone was purchased from Shanghai Chemical Factory. 4-((4-Hydroxyphenyl)diazenyl)benzonitrile, 1,4-phenylenebis((4-fluorophenyl)methanone) (PBFM) and sodium 5, 5′-carbonylbis(2-fluorobenzenesulfonate) were synthesized according to the protocols reported in the literature [25,29]. All other reagents and solvents were obtained commercially and were purified by conventional methods. K_2CO_3 was dried at 120 °C for 24 h before polymerization.

2.2. Synthesis

2.2.1. Synthesis of 5,5′-carbonylbis(2-fluorobenzene-1-sulfonyl chloride) (1)

Dry sodium 5,5′-carbonylbis(2-fluorobenzenesulfonate) (25.34 g, 60 mmol) was mixed with chlorosulfonic acid (63 mL, 540 mmol) under a nitrogen atmosphere. The reaction temperature was kept at 100 °C for 4 h. Then, the mixture was poured into ice-water, neutralized with $NaHCO_3$ and extracted with dichloromethane. The resulting product was recrystallized from toluene to afford pure white crystals. Yield: 75%, mp: 135 °C (determined by DSC); IR (KBr, cm^{-1}): 1385, 1175 (–SO_2Cl); ^1H NMR (DMSO-d_6, δ, ppm): 8.06 (d, J = 6.9 Hz, 2H), 7.73 (m, 2H), 7.34 (t, J = 9.5 Hz, 2H).

2.2.2. Synthesis of bis(4-((4-cyanophenyl)diazenyl)phenyl)5,5′-carbonylbis(2-fluorobenzenesulfonate) (2)

4-((4-Hydroxyphenyl)diazenyl)benzonitrile (14.06 g, 63 mmol) and triethylamine (9.1 mL, 63 mmol) were dissolved in 300 mL dry dichloromethane in a 1000 mL three-necked flask under a nitrogen atmosphere. The solution of 5,5′-carbonylbis(2-fluorobenzene-1-sulfonyl chloride) (12.46 g, 30 mmol) in 300 mL dry dichloromethane was added dropwise into the above mixture, which was then stirred for 12 h at room temperature. After washing with water/acid/water, the dichloromethane was evaporated, and the product was recrystallized from 1,4-dioxane. Orange-red crystals were obtained (21.5 g). Yield: 88%, mp: 233 °C (determined by DSC); MALDI-TOF-MS: $C_{39}H_{22}F_2N_6O_7S_2$ m/z = 790.1 (M^+ + H); IR (KBr, cm^{-1}): 2231 (–CN), 1363, 1196 (Ar–SO_3–Ar); ^1H NMR (DMSO-d_6, δ, ppm): 8.22 (m, 2H), 8.10–8.07 (m, 6H), 8.01–7.96 (m, 8H), 7.84 (t, J = 9.1 Hz, 2H), 7.44 (d, J = 7.7 Hz, 4H); ^{13}C NMR (DMSO-d_6, δ, ppm): 190.91, 162.76, 160.65, 154.68, 151.82, 140.40, 134.72, 134.34, 133.20, 125.80, 124.13, 123.93, 123.52, 119.71, 119.12, 114.59.

2.2.3. Synthesis of di-azobenzene functionalized poly(arylene ether)s (diazo-PAEs) (3)

Monomer 2, PBFM, 6F-BPA, K_2CO_3, N,N-dimethylacetamide (DMAc) and toluene were added to a 100 mL three-necked flask equipped with a mechanical stirrer, a Dean–Stark trap, a condenser, a thermometer and a nitrogen inlet. Under a nitrogen atmosphere, the mixture was heated to 130–140 °C and maintained at that temperature for 3 h to dehydrate the system by means of a Dean–Stark trap through toluene. After dehydration and removal of the toluene, the polycondensation reaction was continued for 10 h at 150 °C. Then, the viscous solution was slowly poured into water and stirred vigorously. The threadlike polymer was pulverized, and the resulting powders were washed several times with hot deionized water and ethanol and dried at 110 °C under vacuum for 24 h (yield: 92%).

2.3. Polymer film preparation

Copolymer films were prepared by the following procedure. Homogeneous solutions of diazo-PAEs in cyclohexanone (10 wt.%) were filtered through 0.8 μm syringe filter membranes. To fabricate SRGs, thin films were obtained via spin-coating the solution onto clean glass substrates. The thickness was controlled to be approximately 1.0 μm by adjusting the spinning rate. For the photoinduced birefringence experiment, films approximately 8.0 μm thick were obtained by solvent-casting on glass substrates. After drying under vacuum for 48 h to drive off the residual solvent, the films were stored in a desiccator until use.

2.4. Measurements

FT-IR spectra (KBr pellet) were recorded on a Nicolet Impact 410 FT-IR spectrophotometer. Gel permeation chromatography (GPC) was carried out using a Waters 410 instrument with tetrahydrofuran (THF) as the eluent and polystyrene as the calibration standard. The inherent viscosity was determined using an Ubbelohde viscometer in a thermostatic container with a polymer concentration of 0.5 g/dL in DMAc at 25 °C. A Bruker 510 instrument was used to record ^1H (500 MHz) and ^{13}C (125 MHz) NMR spectra. Glass transition temperatures (T_gs) were determined by DSC (Model Mettler DSC821^e) at a heating rate of 20 °C/min under a nitrogen atmosphere. Thermo-gravimetric analysis was performed on a Perkin Elmer Pyris 1 TGA analyzer at a heating rate of 10 °C/min under a nitrogen atmosphere. Polarized optical microscopy (POM) was performed on a Leica DLMP with a Linkam THMSE 600 hot stage. UV–visible absorption spectra were recorded on a UV2501-PC spectrophotometer.

2.5. Optical measurements

The experimental setups for the photoinduced birefringence experiments and SRG formation have been described by our group previously [26], and only a few details are given here. Photoinduced birefringence was evaluated using a pump–probe optical configuration. The polarization direction of the pump laser (532 nm 47 mW/cm^2) made a 45° angle with respect to the probe beam (632.8 nm He:Ne laser) polarization. The films were placed between two crossed polarizers (P and A) in the path of the probe laser beam. A birefringence Δn induced by the 532 nm pump laser resulted in transmission of the 632.8 nm probe beam through polarizer A. The birefringence (Δn) value was calculated using $I_t = I_o - \sin^2(\pi \Delta n d/\lambda)$, where I_t is the transmitted probe light intensity at time t, d is the sample thickness, λ is the wavelength of the probe light and I_o is the transmitted probe light intensity for the given polarizer/analyzer orientation (in the absence of the sample). The holographic gratings were optically inscribed on the spin-coated films with p-polarized interfering laser beams. A frequency-tripled, Q-switched, single-mode neodymium dope yttrium aluminum garnet nanosecond laser with a 355 nm wavelength and a 10 ns pulse width (Spectra-physics) was utilized as the recording light source. The output laser light was split into two beams of equal intensity (approximately 40 mW/cm^2), each with a diameter of approximately 10 mm. The surface topology of the films was observed using a Nanoscope atomic force microscope (AFM) in tapping mode.

3. Results and discussion

3.1. Synthesis of monomers

A novel aromatic difluoride monomer containing di-azobenzene groups was designed and synthesized by a two-step reaction, as shown in Scheme 1. First, we prepared monomer 1 via an acid-chloride reaction from sodium 5,5′-carbonylbis(2-fluorobenzenesulfonate) and chlorosulfonic acid. Then, monomer 2 was prepared from monomer 1 and 4-((4-hydroxyphenyl)diazenyl)benzonitrile by esterification. After recrystallization from 1,4-dioxane, orange-red crystals of monomer 2 were obtained with a yield of 88%. The structure of monomer 2 was determined by MS, FT-IR and NMR. As shown in Fig. S1 (in the Supporting information), the assignments of the ^{1}H NMR and ^{13}C NMR signal peaks of monomer 2 correspond well to the expected structure.

3.2. Synthesis of diazo-PAEs

Aromatic poly(aryl ether)s containing pendent di-azobenzene groups (diazo-PAEs) were synthesized by a typical nucleophilic substitution polycondensation reaction from bis(4-((4-cyanophenyl)diazenyl)phenyl)5,5′-carbonylbis(2-fluorobenzenesulfonate) (monomer 2), 4-phenylenebis((4-fluorophenyl)methanone) (PBFM), and 4,4′-(hexafluoroisopropylidene)diphenol (6F-BPA), as shown in Scheme 2. The copolymerization was carried out in DMAc under a nitrogen atmosphere with potassium carbonate as a base catalyst. Toluene was used to dehydrate the reaction system. All obtained polymers showed good solubility in common organic solvents such as chloroform, tetrahydrofuran, N,N-dimethylformamide, N-methyl-2-pyrrolidone and cyclohexanone. From Table 1, it is evident that the number average molecular weights and intrinsic viscosities of the polymers both decreased with increasing azobenzene content due to the lower reactivity of monomer 2. All polymers had number average molecular weights above 1.0×10^4, indicating high molecular weights. The structures of the diazo-PAEs were confirmed using FT-IR, UV–vis and ^{1}H NMR spectra. In ^{1}H NMR spectra (Fig. S2 in the Supporting information), diazo-PAEs 3b–d showed characteristic signals corresponding to the protons of the di-azobenzene groups at around 8.2 (protons H-8) and 7.9–8.1 (protons H-7, H-10, H-11, H-12) ppm, which correspond well with the expected structures. In the FT-IR spectra of 3b–d, the characteristic absorption bands at 2229, 1246, 1379 and 1660 cm^{-1} were attributed to the stretching vibrations of –CN, Ar–O–Ar, Ar–SO_3–Ar and –CO–, which further confirmed the successful preparation of diazo-PAEs 3b–d despite the existence of bulky pendant groups in monomer 2. UV–vis absorption spectra of diazo-PAEs (3a–d) in DMF solution were recorded (Fig. 1). The characteristic absorption bands due to π–π^* and n–π^*, the intramolecular charge-transfer of azobenzene chromophores at around 350 nm and 445 nm, respectively, can be observed in the spectra of 3b–d. The high-energy band at 350 nm is attributed to the *trans*-isomer, whereas the low-energy band at 445 nm is derived from the metastable *cis*-isomer. The absorption intensity of the π–π^* electronic transition of azobenzene chromophores clearly increases with monomer 2 content.

3.3. Thermal properties of diazo-PAEs

DSC and TGA measurements were carried out to investigate the thermal properties of diazo-PAEs. Fig. S3 in the Supporting information shows the DSC curves of polymers 3a–d, and the experimental data are listed in Table 1. The diazo-PAEs 3a–d had glass transition temperatures above 160 °C, and no other thermal change except the glass transition was observed below the decomposition temperature, indicating the amorphous nature of diazo-PAEs. The TGA curves and the data for diazo-PAEs are shown in Fig. S4 (in Supporting information) and Table 1, respectively. The temperatures at 5% weight loss (TGA-5%) of 3a–d were all above 406 °C, indicating excellent thermal stability. From the TGA curve of pure PAE 3a, only one degradation step with the maximum weight loss at 550 °C was observed. Compared to the TGA curve of 3a, the TGA curves of copolymers 3b–d exhibited another degradation step with the maximum weight loss at 408 °C. This extra degradation step can be attributed to the thermal degradation of azobenzene moieties. The 5% weight-loss temperatures of diazo-PAEs decreased from 516 to 406 °C for azobenzene contents from 0% to 60%.

3.4. Photoisomerization behavior of diazo-PAEs

The photoisomerization behavior of the diazo-PAEs 3b–d in DMF solutions was investigated by UV–vis spectroscopy after irradiation with 360 nm UV light. As shown in Fig. 2A, UV–vis spectra of 3b were recorded over different time intervals until the photostationary state was reached (irradiated for 105 s). After irradiation with 360 nm UV light, the absorption intensity of the *trans*-form of azobenzene at 350 nm decreases rapidly, while the intensity of the *cis*-form of azobenzene at 445 nm slightly increases with the irradiation time, indicating the *trans*-to-*cis* photoisomerization of the

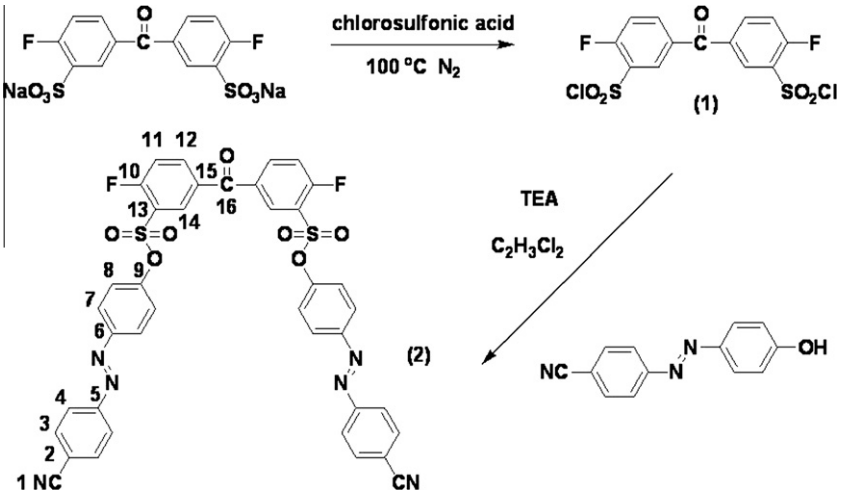

Scheme 1. Synthesis of monomers 1 and 2.

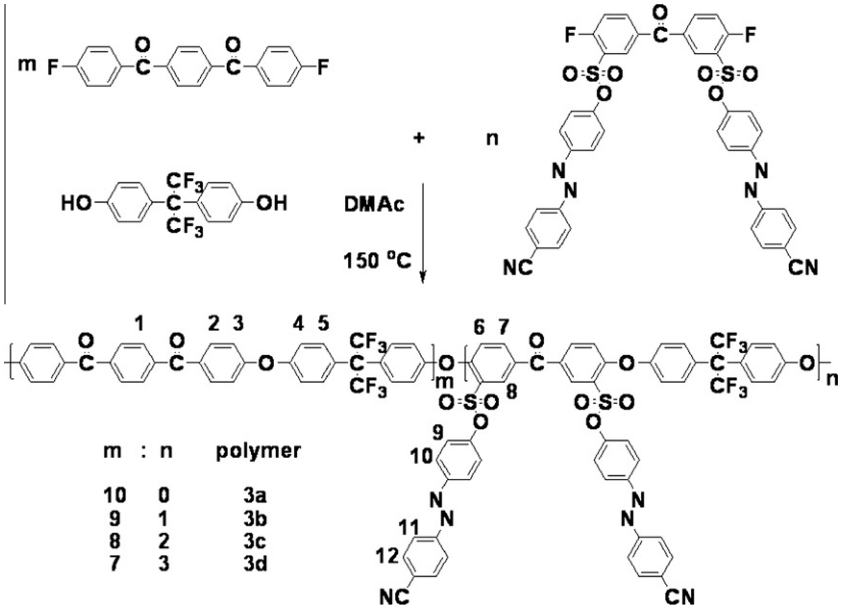

Scheme 2. Synthesis of diazo-PAEs 3–d.

Table 1
Properties of diazo-PAEs.

Polymer	Azo (mol.%)	η^a (dL/g)	$M_n \times 10^4$	M_w/M_n	$T_g{}^b$ (°C)	$T_{d5}{}^c$ (°C)	$T_{d10}{}^d$ (°C)	Modulation-depth (nm)
3a	0	0.66	3.89	2.06	161	516	534	–
3b	20	0.48	1.62	1.69	170	501	528	238
3c	40	0.38	1.23	1.74	163	426	513	258
3d	60	0.50	1.04	1.41	161	406	464	283

[a] Inherent viscosity was determined using an Ubbelohde viscometer in a thermostatic container with a polymer concentration of 0.5 g/dL in DMAc at 25 °C.
[b] Glass transition temperatures were determined by DSC.
[c] 5% Weight-loss temperatures were detected at a heating rate of 10 °C/min in nitrogen with a gas flow rate of 100 mL/min.
[d] 10% Weight-loss temperatures were detected at a heating rate of 10 °C/min in nitrogen with a gas flow rate of 100 mL/min.

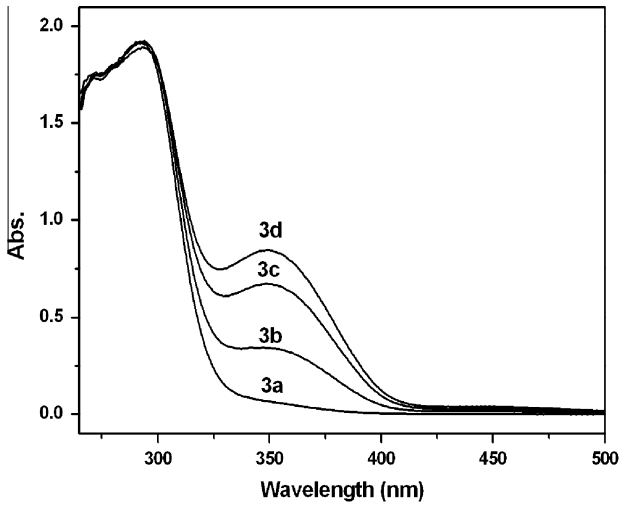

Fig. 1. UV–vis spectra of diazo-PAEs 3a–d in DMF solution.

azobenzene chromophores. Diazo-PAEs 3c and 3d displayed similar photoisomerization behaviors.

The *trans*-to-*cis* photoisomerization rates of diazo-PAEs in DMF solution were analyzed using the UV absorption at 350 nm. The photoisomerization kinetics of diazo-PAEs 3b–d were further studied and are presented in Fig. 2B. It can be seen that ln $((A_\infty - A_t)/(A_\infty - A_0))$ is linearly dependent on time (where A_0, A_t and A_∞ are the absorbances at 350 nm at time 0, time t and the photostationary state, respectively), confirming that the *trans*-to-*cis* photoisomerizations of 3b–d obey first-order kinetics, as reported previously [30]. The slope of the plots of ln $((A_\infty - A_t)/(A_\infty - A_0))$ against time gives the first-order rate constants (k_P) for the *trans*-to-*cis* photoisomerization of diazo-PAEs. The rate constants of the photoisomerization of diazo-PAEs were 0.0210, 0.0253 and 0.0309 s^{-1} for 3b, 3c and 3d, respectively. Copolymer 3b shows the lowest *trans*-to-*cis* photoisomerization rate due to the steric hindrance of the polymer chain configuration [19]. With increases in the content of rigid 1,4-phenylenebis((4-fluorophenyl)methanone), the motion of the azobenzene chromophores becomes difficult, which further restricts the photoisomerization process.

3.5. Photoinduced surface relief grating formation of diazo-PAEs

The formation of photoinduced surface relief gratings is one of the most interesting properties of azo-polymers. Compared with other technologies used to produce topographic gratings, this photo-fabrication approach can be easily completed by a single-step all-optical process. Generally, a 488 nm laser beam is used to fabricate SRGs on azo-polymers [14]. In this study, a 355 nm light was chosen because diazo-PAEs are photoactive to UV light around 350 nm. Compared to a 488 nm laser beam, a shorter wavelength laser beam (355 nm) offers the opportunity to explore the use of these polymers for high-density information storage [26]. Spin-coated films of diazo-PAEs 3b–d with smooth surfaces were obtained on glass substrates and were used for inscription experi-

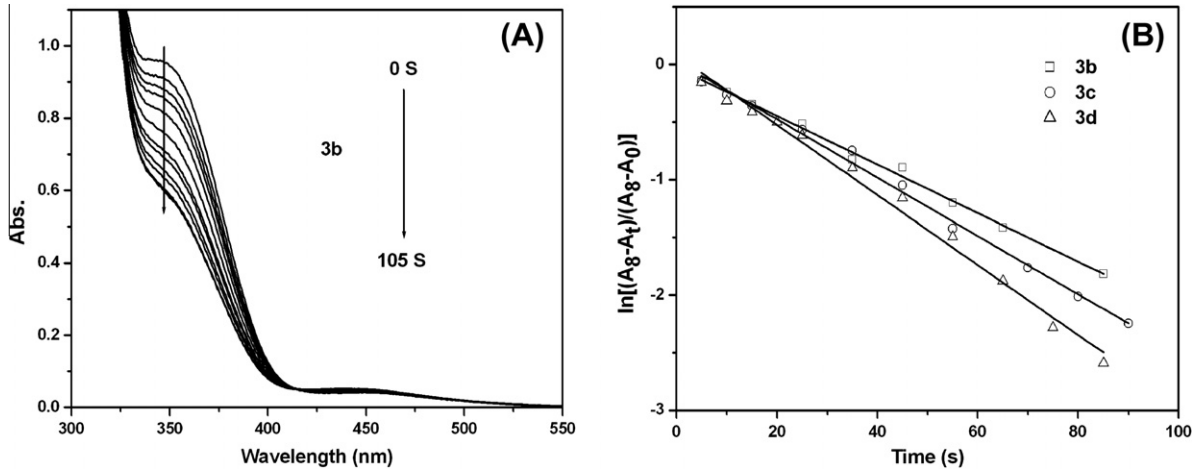

Fig. 2. (A) Changes in the UV–vis absorption spectrum of 3b in DMF solution at 25 °C with different irradiation times under 360 nm light irradiation. (B) First-order *trans*-to-*cis* isomerization kinetics of 3b, 3c and 3d.

ments. The interference pattern of laser beams at 355 nm was produced by two p-polarized beams with incident angles of +11.5° and −11.5°. The films were subsequently exposed to two polarized interfering laser beams of equal intensity (approximately 40 mW/cm^2) for 30 s, and SRGs were sufficiently formed on the films. Fig. 3 shows a typical AFM plane and three-dimensional images of the surface relief structures on the diazo-PAE 3b film. Clear sinusoidal surface relief gratings with regular spacing were observed. AFM section analysis revealed a modulation depth of ca. 238 nm and a grating spacing of ca. 898 nm, as determined by the interference pattern. From Table 1, the following general trend can be observed: under the same irradiation conditions (Irradiation energy: approximately 80 mW/cm^2 and time: 30 s), the relief depth of the gratings increases with the molar fraction of azobenzene units. In addition, the modulation depth could be also adjusted by the irradiation time and the irradiation energy. The grating spacing is equal to the period of the interference pattern (Λ) and can be controlled by adjusting the angle θ between the two interfering beams, according to the equation $\Lambda = \lambda/2\sin(\theta/2)$, where λ is the wavelength of the writing beams [5].

3.6. Thermal stability of the SRGs of 3b

Another important requirement of SRGs is shape stability in terms of long-term storage and durability at high temperature [31]. The thermal stability of SRGs formed on the diazo-PAE 3b film (238 nm) was investigated by polarized optical microscopy (POM). No obvious change in these SRGs was observed when they was heated from room temperature to 170 °C (T_g of 3b) or maintained at 170 °C for 30 min. When the temperature was increased to

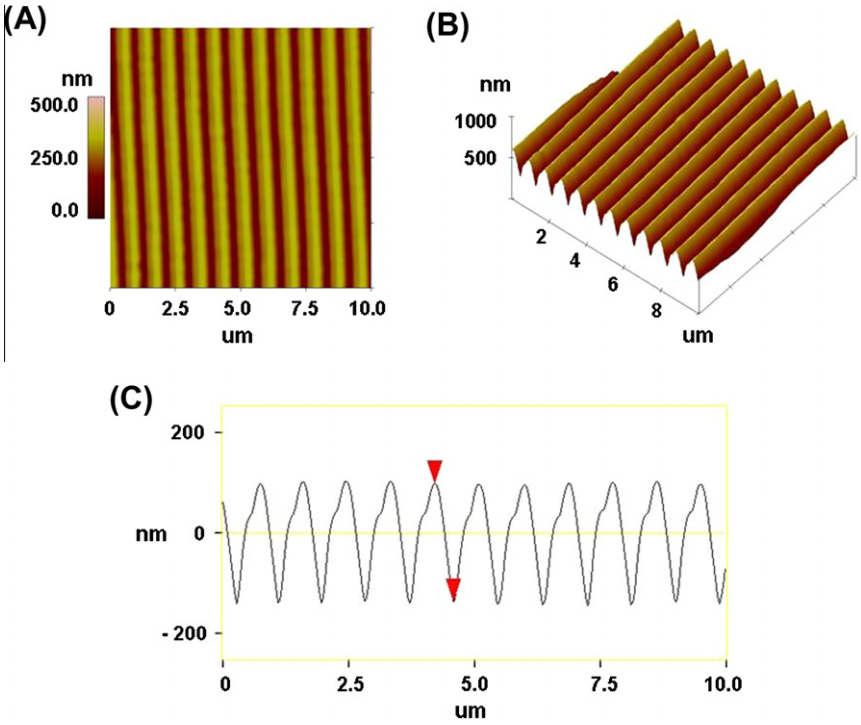

Fig. 3. Images of the typical SRGs formed on diazo-PAE 3b films: (A) AFM plane view of the SRGs (10 × 10 μm^2); (B) typical AFM 3-D view of the SRGs (10 × 10 μm^2); and (C) section analysis of the SRGs.

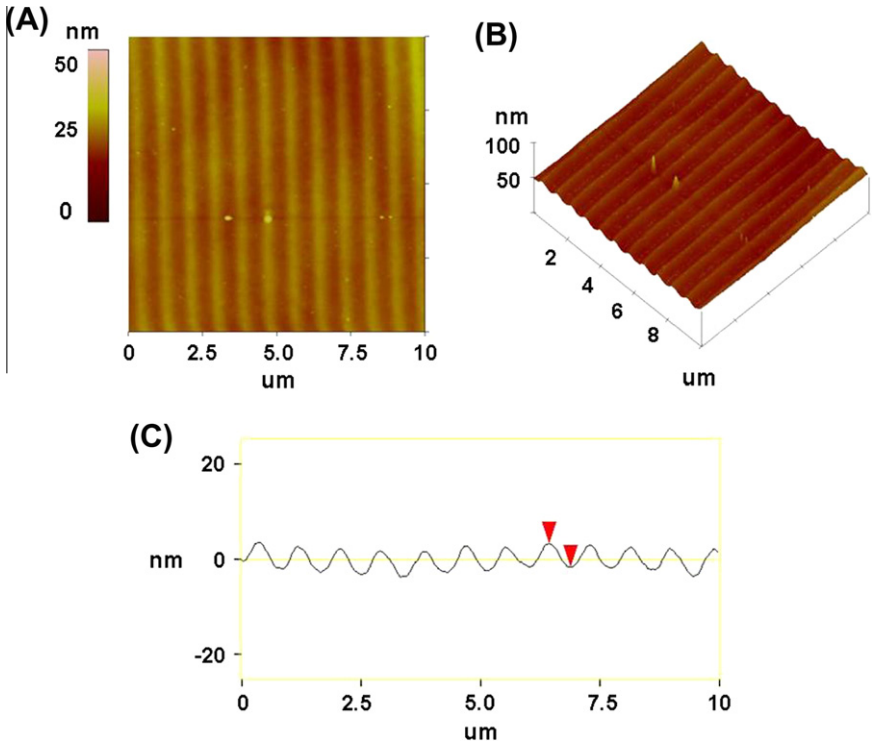

Fig. 4. Images of the typical SRGs formed on diazo-PAE 3b film after heating at 220 °C for 90 min: (A) AFM plane view of the SRGs ($10 \times 10\ \mu m^2$); (B) typical AFM 3-D view of the SRGs ($10 \times 10\ \mu m^2$); and (C) section analysis of the SRGs.

220 °C, SRGs on the diazo-PAE 3b film became slightly blurry, and after heating at this temperature for 90 min, the SRGs almost disappeared. The surface morphology of the diazo-PAE 3b film was further investigated by AFM, as shown in Fig. 4. Although the surface modulation depth decreased from 238 nm to approximately 6 nm after heating at 220 °C for 90 min, the SRGs on the diazo-PAE 3b film still retained a good shape. The excellent stability of SRGs formed on diazo-PAEs will favor their used on future practical applications.

3.7. Photoinduced birefringence of diazo-PAEs

Photoinduced birefringence is another important feature of azo-polymers that makes them suitable for optical storage applications. Herein, the photoinduced birefringence of diazo-PAEs was investigated by exposing diazo-PAE casting-films to a linearly polarized laser beam ('writing' beam) at room temperature. The measured photoinduced birefringence curves of 3b–d as a function of time are shown in Fig. 5A. The moment at which the pump laser was switched on or off is marked with a letter. For copolymer 3b, before irradiation, no optical anisotropy is observed because of the homogeneously random alignment of the azobenzene chromophores. Under irradiation with a linearly polarized 532 nm laser beam (approximately 47 mW/cm^2, at point *A*), birefringence signals were induced immediately and reached approximately 0.1030 due to the alignment of the azobenzene chromophores perpendicular to the pump laser polarization direction through multiple *trans–cis-trans*-isomerization cycles of the azo moieties. The birefringence value exhibited a slight decay after the pump laser was switched off (at point B) because of the thermal isomerization

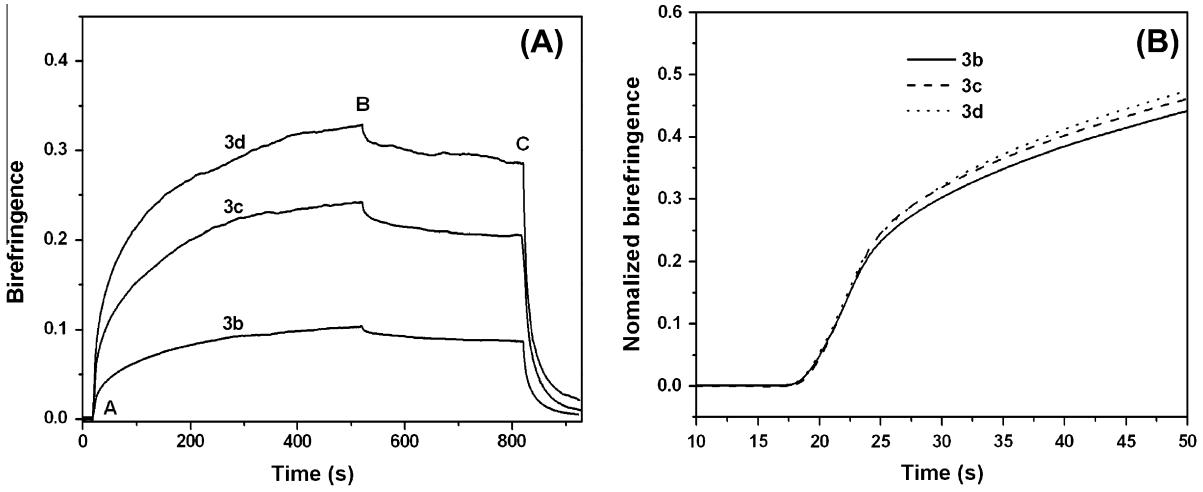

Fig. 5. (A) Typical behavior of the photoinduced birefringence of diazo-PAEs 3b–d at room temperature: at point A, the writing laser was turned on; at point B, the writing laser was turned off; and at point C, the circularly polarized light was turned on. (B) Normalized photoinduced birefringence of the 10–50 s regions.

from cis to trans-form and dipole redistribution, which increase the entropy. However, compared to other azo-polymers [11,32,33], diazo-PAEs show much smaller birefringence decay and possess a remnant value greater than 85% of the saturation value, indicating the excellent stability of the photoinduced orientation. This stability is mainly attributed to the rigidity of the aromatic main chain structures of diazo-PAEs, which suppress the relaxation process of the photoalignment. The remaining photoinduced anisotropy can be erased with a circularly polarized beam ('erasing' beam) (at point *C*). Copolymers 3c and 3d exhibited behaviors similar to those described above (shown in Table 2). From this table, it is evident that the saturation values of diazo-PAEs 3b–d varied from 0.1030 to 0.3289. The remnant values of these polymers varied from 0.0875 to 0.2859. The saturation value and remnant value both increased with increasing azobenzene content.

To allow qualitative comparison of the birefringence evolution with irradiation time for different diazo-PAEs, in Fig. 5B, we show the same evolution, but with the birefringence values normalized to the saturation value [34]. From the growth curves of the three copolymers, it can be seen that the order of the birefringence growth rate was 3d > 3c > 3b. Generally, the growth process of the photoinduced birefringence is attributable to the multiple *trans–cis-trans*-isomerizations of the azobenzene moieties and the reorientation of azobenzene chromophores through these isomerization cycles. Therefore, their birefringence growth rates depend on their photoisomerization rates. As a result, copolymer 3d, which has the fastest photoisomerization rate as discussed in Section 3.4, shows the highest birefringence growth rate among these copolymers.

The complete reversibility of the photoinduced birefringence of diazo-PAEs is related to fatigue resistance properties. As shown in Fig. 6, diazo-PAEs are promising for use in reversible optical storage applications. Indeed, after several irradiation steps with linearly polarized and circularly polarized laser beams alternatively acting on a diazo-PAE 3b film, the saturation values and remnant values were similar. This result indicates that diazo-PAEs have excellent reproducibility, without any degradation of the signal or material fatigue.

Table 2
Photoinduced birefringence characteristics of diazo-PAEs.

Polymer	Saturation value	Remnant value	Remnant value (%)[a]
3b	0.1030	0.0875	85
3c	0.2414	0.2056	85
3d	0.3289	0.2859	87

[a] Remnant value (%) = remnant value/saturation value × 100%.

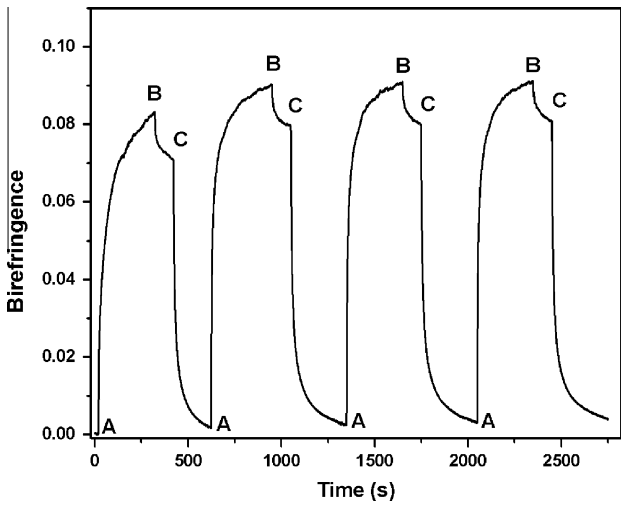

Fig. 6. Multiple writing-erasing cycles of diazo-PAE 3b at room temperature: at point *A*, the writing laser was turned on; at point *B*, the writing laser was turned off; and at point *C*, the circularly polarized light was turned on.

4. Conclusions

A series of di-azobenzene functionalized poly(arylene ether)s (diazo-PAEs) were successfully synthesized via a nucleophilic substitution polycondensation reaction. These polymers exhibit good solubility and thermal stability. Upon irradiation with 360 nm UV light, all diazo-PAEs exhibited obvious photoisomerization behavior in DMF solution due to the existence of azobenzene groups. After exposure to an interference pattern created by 355 nm laser beams, diazo-PAE films rapidly formed thermal-stable surface relief gratings, displaying their potential applications in high-density optical data storage. Upon irradiation with a 532 nm Nd:YAG laser beam, diazo-PAEs presented large, high-quality, photoinduced birefringence with a remnant value greater than 85% of the saturation value. Furthermore, multiple writing/erasing experiments indicate that diazo-PAEs have potential applications in reversible optical storage.

Acknowledgment

The authors gratefully acknowledge the National Science Foundation of China (50803025) for the financial support.

Appendix A. Supplementary data

Supplementary data associated with this article can be found, in the online version, at doi:10.1016/j.reactfunctpolym.2011.01.011.

References

[1] W.M. Gibbons, P.J. Shannon, S.T. Sun, B.J. Swetlin, Nature 351 (1991) 49–50.
[2] S. Hvilsted, C. Sanchez, R. Alcala, J. Mater. Chem. 19 (2009) 6641–6648.
[3] H.R. Hafiz, F. Nakanishi, Nanotechnology 14 (2003) 649–654.
[4] G. Iftime, F.L. Labarthet, A. Natansohn, P. Rochon, J. Am. Chem. Soc. 122 (2000) 12646–12650.
[5] A. Natansohn, P. Rochon, Chem. Rev. 102 (2002) 4139–4175.
[6] Y.W. Bai, N.H. Song, J.P. Gao, X. Sun, X.M. Wang, Z.Y. Wang, J. Am. Chem. Soc. 127 (2005) 2060–2061.
[7] Y.L. Yu, M. Nakano, T. Ikeda, Nature 425 (2003) 145.
[8] D.H. Han, X. Tong, Y. Zhao, T. Galstian, Y. Zhao, Macromolecules 43 (2010) 3664–3671.
[9] P. Rochon, E. Batalla, A. Natansohn, Appl. Phys. Lett. 66 (1995) 136–138.
[10] D.Y. Kim, S.K. Tripathy, L. Li, J. Kumar, Appl. Phys. Lett. 66 (1995) 1166–1168.
[11] Y. Wu, A. Natansohn, P. Rochon, Macromolecules 37 (2004) 6090–6095.
[12] J. Isayama, S. Nagano, T. Seki, Macromolecules 43 (2010) 4105–4112.
[13] N. Zettsu, T. Ogasawara, N. Mizoshita, S. Nagano, T. Seki, Adv. Mater. 20 (2008) 516–521.
[14] R. Walker, H. Audorff, L. Kador, H.W. Schmidt, Adv. Funct. Mater. 19 (2009) 1–9.
[15] M.J. Kim, E.M. Seo, D. Vak, D.Y. Kim, Chem. Mater. 15 (2003) 4021–4027.
[16] E. Ishow, B. Lebon, Y.N. He, X.G. Wang, L. Bouteiller, L. Galmeche, K. Nakatani, Chem. Mater. 18 (2006) 1261–1267.
[17] J. Gao, Y.N. He, H.P. Xu, B. Song, X. Zhang, Z.Q. Wang, X.G. Wang, Chem. Mater. 19 (2007) 14–17.
[18] J. Vapaavuori, A. Priimagi, M. Kaivola, J. Mater. Chem. 20 (2010) 5260–5264.
[19] X.Q. Xue, J. Zhu, Z.B. Zhang, N.C. Zhou, X.L. Zhu, React. Funct. Polym. 70 (2010) 456–462.
[20] E. Schab-Balcerzak, M. Siwy, M. Kawalec, A. Sobolewska, A. Chamera, A. Miniewicz, J. Phys. Chem. A 113 (2009) 8765–8780.
[21] J.B. Rose, Polymer 15 (1974) 456–465.
[22] H.B. Zhang, J.H. Pang, D. Wang, X. Li, Z.H. Jiang, J. Membr. Sci. 264 (2005) 56–64.
[23] X.B. Chen, B.J. Liu, H.B. Zhang, S.W. Guan, J.J. Zhang, Z.H. Jiang, Langmuir 25 (2009) 10444–10446.
[24] J.J. Zhang, H.B. Zhang, X.B. Chen, Y.H. Zhang, X.F. Li, Z.H. Jiang, Mater. Lett. 64 (2010) 337–340.

[25] X.B. Chen, J.J. Zhang, H.B. Zhang, Z.H. Jiang, G. Shi, Y.L. Song, Dyes Pigments 77 (2008) 223–228.
[26] X.B. Chen, Y.H. Zhang, B.J. Liu, J.J. Zhang, H. Wang, Z.H. Jiang, J. Mater. Chem. 18 (2008) 5019–5026.
[27] X.Y. Jiang, X.B. Chen, X.G. Yue, J.J. Zhang, S.W. Guan, H.B. Zhang, W.Y. Zhang, Q.D. Chen, React. Funct. Polym. 70 (2010) 616–621.
[28] X.Y. Jiang, H. Wang, X.B. Chen, X.J. Li, J.X. Mu, S.L. Zhang, React. Funct. Polym. 70 (2010) 699–705.
[29] F. Wang, T.L. Chen, J.P. Xu, Macromol. Chem. Phys. 199 (1998) 1421–1426.
[30] G.S. Kumar, D.C. Neckers, Chem. Rev. 89 (1989) 1915–1925.
[31] N. Zettsu, T. Ubukata, T. Seki, K. Ichimura, Adv. Mater. 13 (2001) 1693–1697.
[32] C. Chun, M. Kim, D. Vak, D.Y. Kim, J. Mater. Chem. 13 (2003) 2904–2909.
[33] R. Fernandez, I. Mondragon, P.A. Oyanguren, M.J. Galante, React. Funct. Polym. 68 (2008) 70–76.
[34] P. Forcén, L. Oriol, C. Sánchez, R. Alcalá, S. Hvilsted, K. Jankova, J. Loos, J. Polym. Sci. Pol. Chem. 45 (2007) 1899–1910.